Supplementary information

Surface Water Retardation around Single-Chain Polymeric Nanoparticles: Critical for Catalytic Function?

Patrick J. M. Stals,[a,b,c,#] Chi-Yuan Cheng,[d,#] Lotte van Beek,[a,d] Annelies C. Wauters,[a,d] Anja R. A. Palmans,[a,b] Songi Han*[,d,e] and E. W. Meijer*[,a,b]

Materials

All commercial reagents and solvents were obtained from Acros, Biosolve, or Sigma-Aldrich, except for deuterated chloroform and deuterated 2-propanol, which were purchased from Cambridge Isotopes Laboratories. Oligo(ethylene glycol) methacrylate (*o*EGMA, M_n = 475 g/mol) was passed through a short column filled with inhibitor remover (Sigma-Aldrich) before use. AIBN was recrystallized from methanol. All other commercial reagents and solvents were used without any additional purification. 4-Cyano-4-methyl-5-(phenylthio)-5-thioxopentanoic acid was kindly provided by SyMO-Chem (Eindhoven, The Netherlands). Azides **1**,[1] **2**,[2] and **3**[3] and 3-(trimethylsilyl)propargyl methacrylate[4] were prepared according to previously described literature procedures. The synthesis of reference polymer **P5** (*DP* = 323) was reported elsewhere.[5] *N*-((1H-Benzo[α]imidazole-2-yl)methyl-1-(pyridin-3-yl methyl)methanamine was kindly provided by dr. S. I. Presolski (Eindhoven University of Technology).

Methods of Polymer Structural Characterization

NMR spectra were measured on a Varian Mercury Vx 400 MHz and/or a Varian 400MR 400 MHz (400 MHz for ^{1}H NMR and 100 MHz for ^{13}C NMR). Deuterated solvents used are indicated in each case. ^{1}H chemical shifts are reported in ppm downfield from tetramethylsilane (TMS). Circular dichroism measurements were performed on a Jasco J-815 spectropolarimeter where the sensitivity, time constant and scan rate were chosen appropriately. In all experiments, the linear dichroism was also measured and in all cases no linear dichroism was observed. Cells with an optical path length of 0.5 cm were used. Dialysis was performed in Spectra/Por Dialysis membranes (Spectrum Laboratories), with a molecular weight cutoff of 6-8 kDa. DMF-SEC measurements were carried out in PL-GPC-50 plus from Polymer Laboratories (Varian Inc. Company) equipped with a refractive index detector and working in DMF containing 10 mM LiBr at 50 °C (flow rate: 1 mL min^{-1}) on a Shodex GPC-KD-804 column (exclusion limit = 400 kDa.; 0.8 cm i.d. × 300 mm) or on a Shodex GPC-KD-805 column (exclusion limit = 5000 kDa.; 0.8 cm i.d. × 300 mm) which were calibrated with poly(ethylene oxide) (PEO) samples (Polymer Laboratories). Dynamic light scattering measurements were performed using a Nano-Series Zetasizer (Nano-ZS ZEN3600, Malvern Instruments, Worcestershire, United Kingdom). IR spectra were recorded on a Perkin-Elmer FRIR Spectrum 2 equipped with a Perkin-Elmer UATR Two accessory.

EPR and ODNP measurements

A polymer concentration of 540 μM (corresponding to approximately 5.4 mM spin label concentration) was used for the ODNP and EPR measurements. Both EPR and ODNP measurements were performed at room temperature. Deuterated 2-propanol was used to avoid proton NMR signal other than water proton to be detected by ODNP. Continuous-wave (cw) EPR spectra were acquired using a standard cylindrical TE_{011} resonator (ER 4119HS-LC, Bruker, Billerica, MA) equipped by a Bruker EMX EPR X-band spectrometer at room temperature. The conventional EPR spectra were acquired using 20 mW microwave power and 100 kHz field modulation with an amplitude of 2 Gauss. The field scan was 10 mT with field centre of 348.5 mT. 1024 data points were recorded with a time constant of 20 ms and the scan rate was 11.4 mT/min.

For ODNP measurements, liquid samples were loaded into a 0.6 mm i.d. 0.84 mm o.d. quartz capillary and both ends were sealed with capillary wax. The capillary was loaded into a homebuilt NMR probe and placed inside a Bruker X-band EPR resonator (ER 4119HS-LC, Bruker, Billerica, MA). EPR spectra were first acquired to determine the center field with a Bruker EMX spectrometer. ^{1}H NMR measurements were performed using a Bruker Avance 300 NMR spectrometer. The magnetic field for ODNP experiments was 0.35 T. During the ODNP measurements, the samples

were continuously irradiated at the EPR frequency by a home-built 8–10 GHz microwave amplifier. T_1 measurements were conducted by a typical inversion-recovery pulse sequence in a 0.35 T electromagnet. Cooling air was flowed over the sample to avoid sample heating during the measurement. The detailed description of ODNP can be found in the literature.[6,7]

Overview of the Overhauser Dynamic Nuclear Polarization (ODNP) method.

ODNP relies on the polarization transfer from the electron spins of the nitroxide radicals to the ^{1}H nuclei of the locally interacting water molecules through dipolar interaction.[8,9] The time-dependent mathematical description of ODNP in liquids is

$$\frac{dI_z}{dt} = -\left(\rho + T_{10}^{-1}\right)\left(I_z - I_0\right) - \sigma\left(S_z - S_0\right) \quad [1]$$

where I and S refer to nuclear and electron spins, I_0 and S_0 are their Boltzmann equilibrium values, T_{10}^{-1} is the nuclear spin relaxation rate resulting from all other mechanism not to paramagnetic relaxation. The self-relaxation rate and cross-relaxation rate are defined as $\rho = w_0 + 2w_1 + w_2$ and $\sigma = w_2 - w_0$, respectively, where w_0, w_1 and w_2 are nuclear-electron zero-, single-, and double-quantum transition rates. The steady-state solution of Eq.[1] under continuous microwave (MW) irradiation at the allowed electron spin transition frequency leads to the NMR signal enhancement

$$E = \frac{\langle I_z \rangle}{I_0} = 1 - \xi f s \left|\frac{\gamma_e}{\gamma_H}\right| = 1 - \left(\frac{w_2 - w_0}{w_0 + 2w_1 + w_2}\right)\left(\frac{w_0 + 2w_1 + w_2}{w_0 + 2w_1 + w_2 + T_{10}^{-1}}\right) s \left|\frac{\gamma_e}{\gamma_H}\right| \quad [2]$$

where ξ is the coupling factor, f is the leakage factor, s is the saturation factor, and γ_e and γ_H are the gyromagnetic ratios of the electron and ^{1}H, given $\left|\gamma_e/\gamma_H\right|$=658. Ideally, s is approaching 1 for a fully saturated electron spin transition. The coupling factor ξ describes the efficiency of cross-relaxation between the electron and ^{1}H spins, which is defined by $\xi = \sigma/\rho$. The coupling factor carries the information of the relative dynamics between the ^{1}H spins of water and the electron spins of the nitroxide radical, and is therefore the quantity of interest. The leakage factor f accounts for the nuclear spin lattice relaxation originating from the interaction with electron spins compared to all other contributing mechanisms, yielding $f = 1 - T_1/T_{10}$, where T_1 and T_{10} are the ^{1}H longitudinal relaxation time in the presence and absence of the radical, respectively. By extrapolating to infinite MW power, the maximal signal enhancement E_{max} can be determined. The saturation factor s can be extrapolated to maximal saturation $s_{max} \approx 1$, which is a valid approximation for slow tumbling macromolecules or assemblies, such as proteins or lipid vesicles studied here.[9,10] The coupling factor can then be determined from Eq. [2]. It is noted that ξ is field dependent. Here, we study the hydration dynamics in polymer systems using ODNP at a magnetic field of 0.35 T, yielding a Larmor frequency for the electron spin of ω_e= 9.8 GHz and for the ^{1}H spin of ω_H= 14.8 MHz. For small molecules in solution, an extreme motional narrowing regime is approached at 0.35 T, yielding $\omega_H\tau \ll \omega_e\tau \ll 1$, where τ is the translational correlation time of the solvent molecules in solution (i.e. we focus on water here). Thus, the coupling factor at this field is modulated by the molecular dynamics of water dipolar coupled with the spin label, whose motional modes on the order of ω_e. In this regime, the closer the correlation time τ of water with respect to the spin label nearby is to 100 ps ($\approx 1/\omega_e$), the more effectively will it modulate the coupling factor. Therefore, ODNP at 0.35 T is extremely sensitive to motion dictated by the translation correlation time τ of water on the tens of up to 1000 ps timescale, covering a wide motional range of water in hydrated macromolecules and soft matter, from the weakly coupled water on the biological surfaces to deeply buried sites in the core of biomacromolecules or their assemblies.[11-15]

In order to quantify the τ value from ξ, the appropriate model governing the dynamic parameters of the solvent molecules interacting with the spin labels has to be applied. For nitroxide radicals free in water, as well as nitroxide radicals tethered on the surface of liposomes, the force-free hard-sphere model[16] has been shown to give a good fit to field cycling relaxometry data[6,7,17] and can be used to model the spectral density function. This method becomes especially convenient, when translation diffusion is the dominant modulator of the electron spin-mediated nuclear spin relaxation that is driven via dipolar coupling between the electron and ^{1}H nuclear spins. This model can be employed in our systems as freely diffusing water interacts with the radicals incorporated on the surface of macromolecules.[11-15] In this case, the coupling factor is given by

$$\xi = \frac{6J(\omega_e + \omega_H,\tau) - J(\omega_e - \omega_H,\tau)}{6J(\omega_e + \omega_H,\tau) + 3J(\omega_H,\tau) + (\omega_e - \omega_H,\tau)}$$

[3]

with following spectral density function[16]

$$J(\omega,\tau) = \frac{8\tau}{27b^3} \frac{1 + \frac{5\sqrt{2}}{8}(\omega\tau)^2 + \frac{1}{4}\omega\tau}{1 + (2\omega\tau)^{1/2} + \omega\tau + \frac{\sqrt{2}}{3}(\omega\tau)^{3/2} + \frac{16}{81}(\omega\tau)^2 + \frac{4\sqrt{2}}{81}(\omega\tau)^{5/2} + \frac{1}{81}(\omega\tau)^3}$$

[4]

where b is the distance of the closest approaches between electron and ^{1}H spins. The Eq.[3] and Eq.[4] enable the determination of thevaluewhich is inversely proportional to local water diffusivity (i.e. $\tau \propto D^{-1}$). In order to compare water diffusivity in different local environments, we introduce the retardation factor, τ/τ_{bulk}, which is the ratio of τ-value of hydration water to that of bulk water, τ_{bulk}. The retardation factor is typically 2-5 for hydration water on water-exposed surfaces of protein or lipid membrane[18,19], whereas it is around 5-11 in the bilayer interior of lipid assemblies.[12,15] However, the relatively modest retardation factor for water within the lipid bilayer only reports on the relatively fast diffusion dynamics of the highly sparse water molecules across the bilayer, but does not provide any information about water content.[12] It is necessary to clarify that we assume a full exchange of water molecules between hydration layer and bulk water within the timescale of ODNP build-up time that is on the order of the T_1 of water protons (i.e. few seconds), so that no pool of unenhanced bulk water skews the ODNP-derived local hydration dynamics. The timescale for the exchangeable protons between water molecules and lipid bilayer surface around the nitroxide radicals is on the order of milliseconds to sub-seconds, so that a full exchange between the surface and bulk water populations is ensured[11], while it is too long to directly influence the timescales of water diffusion at tens to hundreds of ps derived by ODNP at 0.35 T. Therefore, the exchangeable protons should have no influence on our ODNP results.

In addition to the standard analysis of ξ, we can separately determine local water mobility at fast timescale (ps) and at slow timescale (ns) using the relaxivity at the electron and ^{1}H Larmor frequency, respectively.[7,20] Typically, the hydration dynamics at several ns or longer timescales is contributed from bound water, whereas hydration dynamics at ps timescale is contributed from loosely bound and freely diffusing water at or near molecular interfaces. This analysis is model-independent and permits the direct comparison of different classes of hydration waters in different local environments. However, it does not easily yield an explicit value for τ as with the standard analysis. k_σ is the cross-relaxivity between electron and ^{1}H spins driven by electron spin-flip excitation at ω_e at a known spin-labeled concentration C_{SL}.

$$k_\sigma = \frac{1 - E_{max}}{C_{SL} T_1} \left|\frac{\gamma_H}{\gamma_e}\right|$$

[5]

Therefore, k_σ is exclusively sensitive to characteristics of fast water diffusion of loosely bound water at tens of ps to sub-ns timescale. On the other hands, k_ρ is the self-relaxivity, which represents the paramagnetic contributions to T_1 relaxation rates of water driven by dipolar self-relaxation of water protons:

$$k_\rho = \frac{T_1^{-1} - T_{10}^{-1}}{C_{SL}} \quad [6]$$

Both k_σ and k_ρ relaxivities probe the values of the spectral density function for fluctuations in dipolar relaxation between electron and ^{1}H. Since $\omega_H \ll \omega_e$, the relaxivities can be approximated as follows.

$$k_\sigma = 6J(\omega_e + \omega_H,\tau) + J(\omega_e - \omega_H,\tau) \approx 5J(\omega_e,\tau) \quad [7]$$

$$k_\rho = 6J(\omega_e + \omega_H,\tau) + 3J(\omega_H,\tau) + J(\omega_e - \omega_H,\tau) \approx 7J(\omega_e,\tau) + 3J(\omega_H,\tau) \quad [8]$$

The coupling factor can then be approximated

$$\xi = \frac{\sigma}{\rho} = \frac{C_{SL} k_\sigma}{C_{SL} k_\rho} \approx \frac{5J(\omega_e,\tau)}{7J(\omega_e,\tau) + 3J(\omega_H,\tau)}$$

[9]

To extract the relaxivity that only depends on the value of the spectral density function for fluctuations of dipolar relaxation at ω_H, the contribution from fast waters (k_σ) can be subtracted from the self-relaxivity (k_ρ) as follows[7], based on Eq.[7] and Eq.[8]:

$$k_{low} \approx \frac{5}{3}k_\rho - \frac{7}{3}k_\sigma \approx 5J(\omega_H,\tau) \quad [10]$$

which is strongly weighted by bound water to the polymer chain moving at slower motion timescale (few ns). Thus, the contribution of slow or bound water diffusing at slower timescale (i.e. $1/\omega_H$ ~ 6.7 ns at 0.35T) can be determined by k_{low}. Recent hardware developments for ODNP have further improved the reliability for quantifying local surface hydration dynamics at 0.35 T. The reproducibility of the ODNP data are presented in Table S1.

In this work, we focus on ODNP measurements at 0.35 T and 9.8 GHz MW frequency that represents an appropriate timescale to probe the translational dynamics of hydration water moving with correlation times on the order of few ps to sub-ns. Specifically in this manuscript, we extract the value for $\tau_{polymer}$ from the coupling factor, ξ, from equations [3] and [4], which represents the translational correlation time of water molecules within 5-10 Å of the nitroxide radical-based spin label tethered on the polymer surface. This value is inversely proportional to the local diffusion coefficient of water if the distances of closest approach between the spin label and water remains constant. The contribution of water that is freely diffusing near the polymer vs. bound to the polymer for a comparable or longer than the tumbling time of the protein can be separately evaluated by relying on a detailed analysis of the ODNP data to extract both the $k_{\sigma,\,polymer}$ and $k_{low,\,polymer}$ relaxitivies, which corresponds to the $k_\sigma$and k_{low} parameters defined in equation [7] and [10], respectively, as well as in the literature[20,21]

Overview of the Electron Paramagnetic Resonance (EPR) method.

The continuous wave (cw) EPR lineshapes were analyzed by spectral simulation using a single-component model, where a MOMD (microscopic order macroscopic disorder) model was used as previously described for the anisotropic motion of the nitroxide radical.[22,23] The detail description of the MOMD model can be found in literature.[24] For all ESR spectral fits in this work, the values of the magnetic tensors *A* and *g* were used as constraints, which were previously determined for R1 spin label in protein systems.[25] These values are A_{xx} = 6.2, A_{yy} = 5.9, A_{zz} = 37.0, and g_{xx} = 2.0078, g_{yy} = 2.0058, g_{zz} = 2.0022.

In this work, we assumed three rotational diffusion tensor, R_x, R_y and R_z are rapidly rotating and have isotropic motion, yield $\langle R\rangle = R_x = R_y = R_z$. In the simulation process, the rotational diffusion constant (*R*) is the only fit parameter. Rotational correlation time (τ_R) was calculated using $\tau_R = 1/(6R)$. To get the best fit, a single-component EPR spectrum with single fit parameter (*R*) was initially fit. Once the *R* value was optimized, the Gaussian inhomogeneous broadening was allowed to vary slightly in order to obtain the best fit. The quality of fit was visually evaluated using the difference between the experimental and theoretical spectra.

Table S1 ODNP parameter for polymer samples, **P2**, **P3**, and **P4**, and control sample using 4-hydroxyl-TEMPO at various 2-propanol concentrations.

Samples	2-propanol (v/v%)	τ (ps)	k_σ ($M^{-1}s^{-1}$)	k_{low} ($M^{-1}s^{-1}$)
P2	0	306±3	36.5±0.4	1138.5±1.0
	15	298±11	41.5±2.3	1239.7±5.4
	30	327±13	52.0±2.7	1792.3±6.4
	50	258±4	57.1±1.2	1376.4±2.9
P3	0	238±2	53.7±0.4	1150.5±1.2
	15	232±2	52.3±0.5	1081.6±1.2
	30	290±3	59.5±0.8	1710.2±2.1
	50	227±4	63.0±3.4	1256.3±8.2
P4	0	188±5	71.3±2.2	1097.2±5.1
	15	203±2	70.5±0.7	1205.2±1.6
	30	214±2	77.6±1.0	1430.4±2.4
	50	216±5	62.5±1.8	1165.0±4.2

Control	0	61±3	92.4±2.9	394.4±6.9
	15	70±5	94.2±4.0	455.7±9.4
	30	95±5	118.0±4.7	780.4±11.0
	50	114±3	115.5±2.9	936.9±7.2

Synthesis of polymers P1-P4.

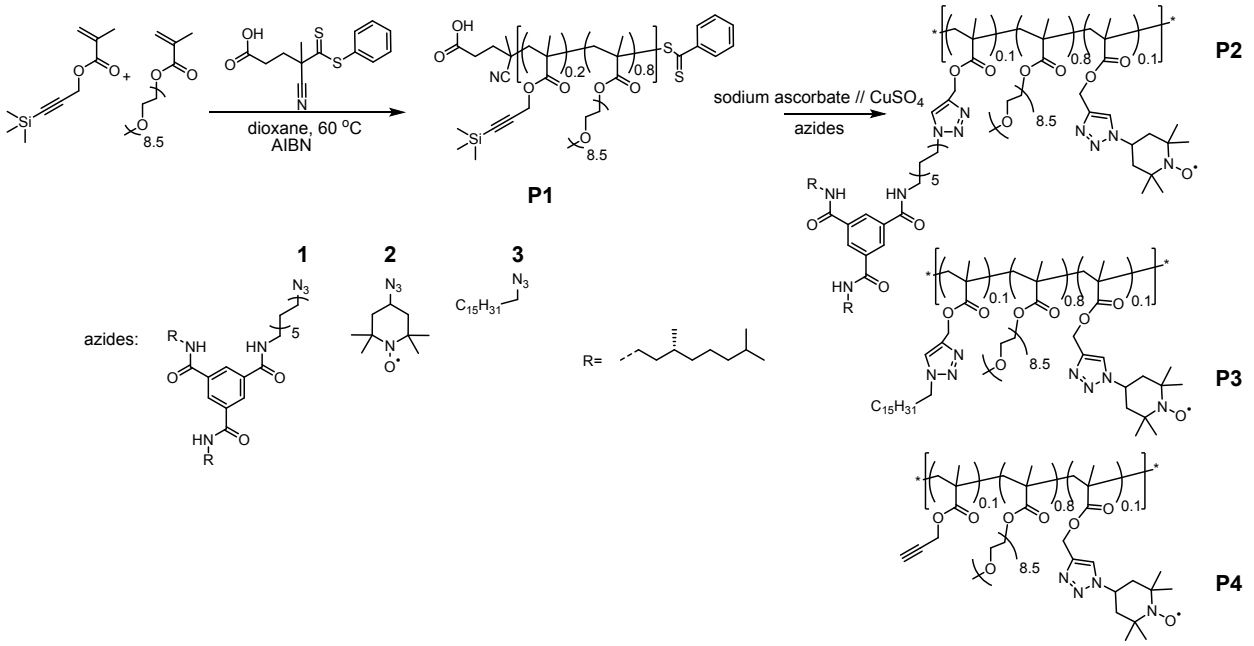

Scheme S1 Synthesis of polymers **P1**-**P4**.

Synthesis of P1: In a Schlenck-flask, *o*EGMA (9.50 g, 20.0 mmol), 3-(trimethylsilyl)propargyl methacrylate (0.982 g, 5.00 mmol), 4-cyano-4-methyl-5-(phenylthio)-5-thioxopentanoic acid (CTA, 1/293 eq. to monomers; 23.79 mg, 85.3 µmol) and azobis(isobutyronitrile) (AIBN, 0.2 eq. to CTA, 2.74 mg, 16.7 µmol) were dissolved in dioxane (50 mL). The mixture was subjected to three freeze-pump-thaw cycles, backfilled with argon and placed in a preheated oil-bath at 60°C. After 46 h, the conversion was determined with ^{1}H-NMR (87%) and the polymerization was stopped by placing the reactor in a liquid-nitrogen bath. The polymer was purified by dialysis in THF and subsequently dried under high vacuum at room temperature to a constant weight to obtain a pink sticky material. M_n and $Đ$ were determined by DMF-SEC relative to PEO-standards. ^{1}H NMR ($CDCl_3$): δ = 4.59 (s broad, O-CH_2-C≡C), 4.08 (s, broad, CO_2-CH_2), 3.65 (s, broad, CH_2-O-CH_2), 3.54 (s, broad, CO_2−CH_2−CH_2−O), 3.37 (bs, O-CH_3), 2.10-0.67 (m, CH, CH_2, CH_3, backbone), 0.19 (s, Si-CH_3); $M_{n,NMR}$ = 107 kDa, DP = 255. SEC: Mn$_{,SEC}$ = 24.6 kDa, $Đ$ = 1.90.

General procedure for synthesis of P2-P4: In a Schlenck-tube, **P1** (200 mg), the first azide (0.048 mmol) and a second azide (0.048 mmol; not applicable for **P4**) were dissolved in DMSO (3 mL). *N*-((1H-Benzo[α]imidazole-2-yl)methyl-1-(pyridin-3-yl methyl)methanamine (6.23 mg, 18.9 µmol) was dissolved in 0.5 mL DMSO and added to the polymer solution. $CuSO_4$ (1.5 mg, 9.4 µmol) and sodium ascorbate (18.6 mg, 9.5 µmol) were dissolved in 4 mL demi water and also added the polymer solution. The mixture was flushed with argon for 1 h, the tube was capped and the mixture was stirred at room temperature for 48 h. Thereafter, the mixture was poured into a beaker filled with 75 mL CH_2Cl_2. To this, 60 mL of a Na_2EDTA solution (1 mM in water) were added and the resulting mixture was stirred for 1 h. The mixture was transferred to a separation funnel, separated and the water layer was extracted once more with 75 mL CH_2Cl_2. The organic layers were collected, concentrated and the polymer was purified with dialysis in EtOH.

P2. Amounts of reactants used: azide **1** = 32.78 mg, 0.048 mmol; azide **2** = 9.47 mg, 0,048 mmol. Yield: 80 mg. Mn$_{,SEC}$ = 30.7 kDa, $Đ$ = 2.80.

P3. Amounts of reactants used: azide **3** = 12.84 mg, 0.048 mmol; azide **2** = 9.47 mg, 0,048 mmol. Yield: 175 mg. Mn$_{,SEC}$ = 29.7 kDa, $Đ$ = 1.90.

P4. Amounts of reactants used: azide **2** = 9.47 mg, 0,048 mmol. Yield: 160 mg. Mn$_{,SEC}$ = 31.5 kDa, $Đ$ = 1.62.

Supporting Figures

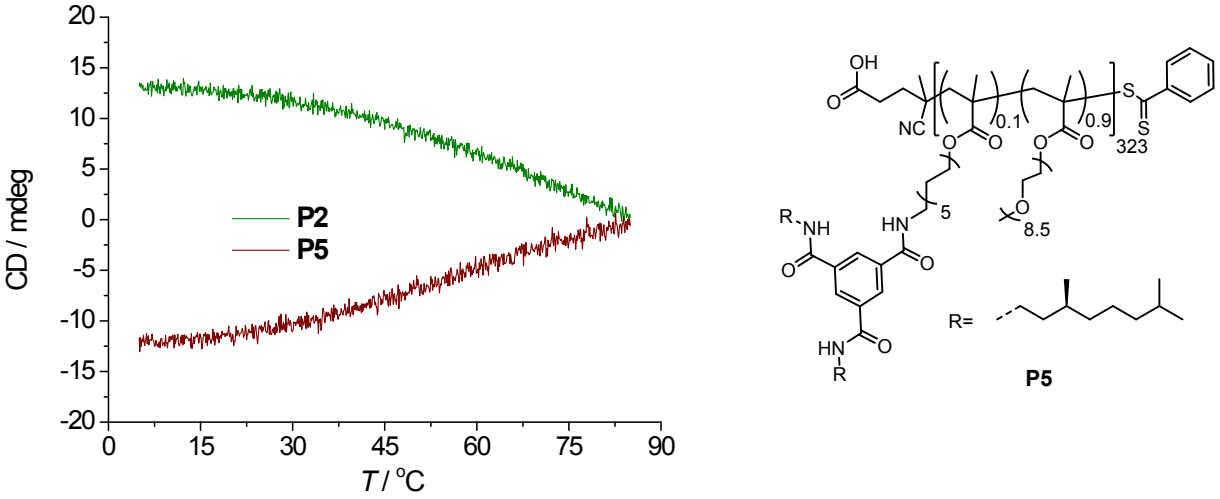

Figure S1 Temperature-wavelength scan measured at a cooling rate of 60 K h^{-1} at λ = 223 nm for solutions of **P2** and **P5** in water (c_{BTA} = 50 µM, l = 0.5 cm); data for **P5** was retrieved from reference 5. Please note that **P2** has the opposite chirality of **P5**. Also, please note that **P3** does not have a CD-probe, but DLS studies showed no temperature-dependent folding behavior.[26]

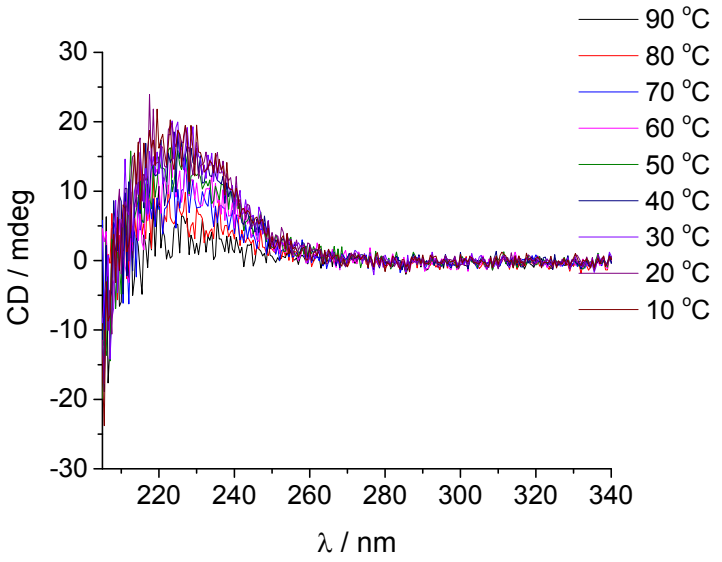

Figure S2 CD-spectra of **P2** in water (c_{BTA} = 50 µM, l = 0.5 cm) at selected temperatures.

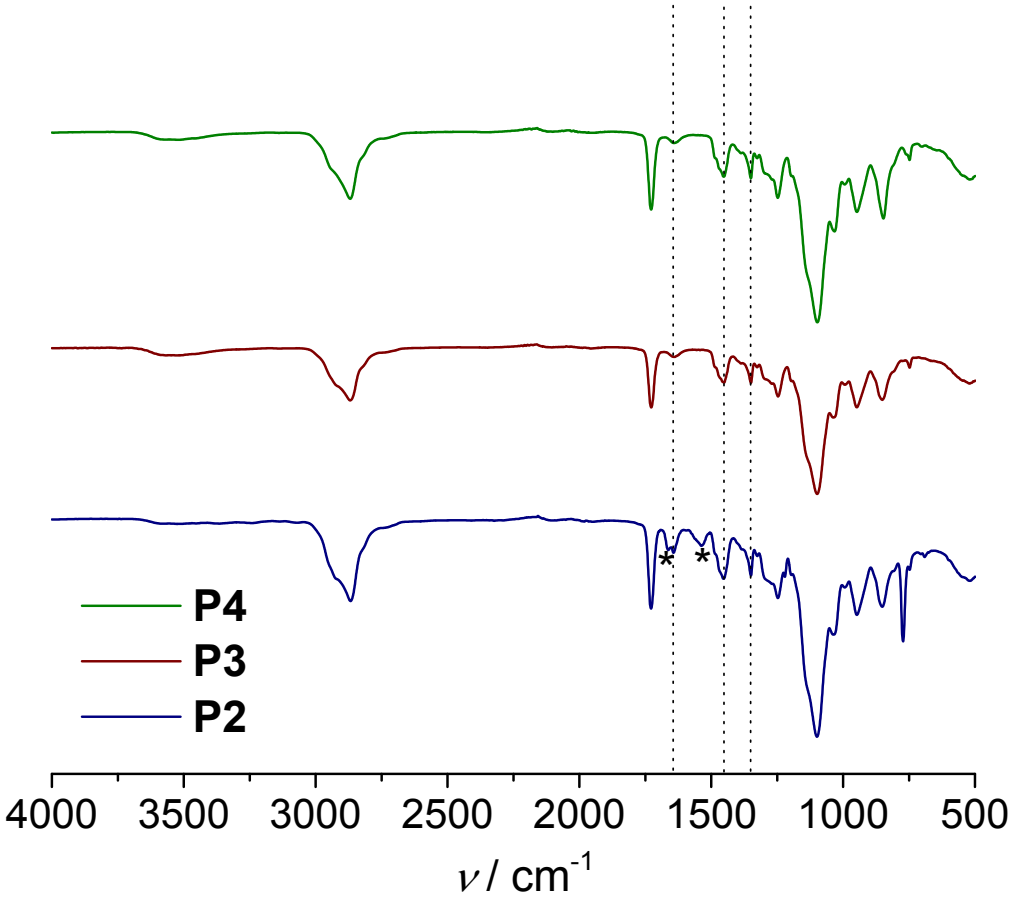

Figure S3 Representative IR spectra for purified **P2**, **P3** and **P4**; no azide functionality is present at 2160-2120 cm^{-1}, while the dotted line at 1350 cm^{-1} is indicative for a nitroxide vibration.[27] The peaks at 1640 cm^{-1} and 1450 cm^{-1} are indicative for triazole ring vibrations,[28] while the peaks denoted with a star (at 1660 cm^{-1} and 1540 cm^{-1}) are indicative for the carbonyl vibration and amide II vibration originating from the presence of the amides of benzene-1,3,5-tricarboxamides.[29]

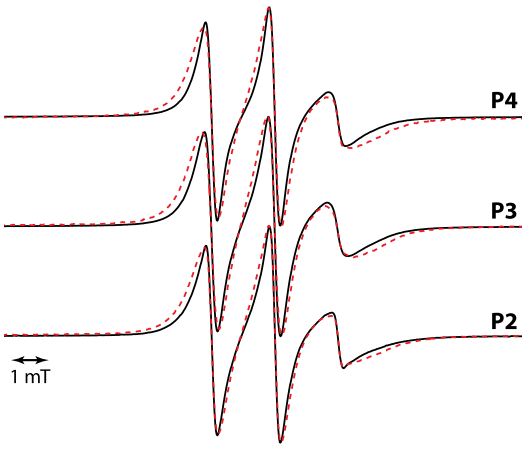

Figure S4 EPR spectra of **P2**-**P4** in the absence (black line) and presence (red dashed line) of 30 wt % sucrose.

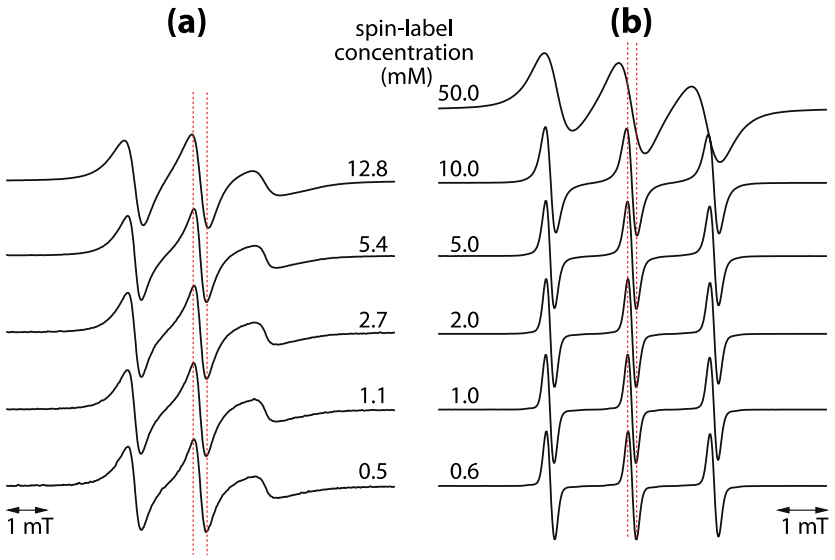

Figure S5 EPR spectra of (a) **P2** (b) 4-hydroxyl-TEMPO at various spin-label concentrations.

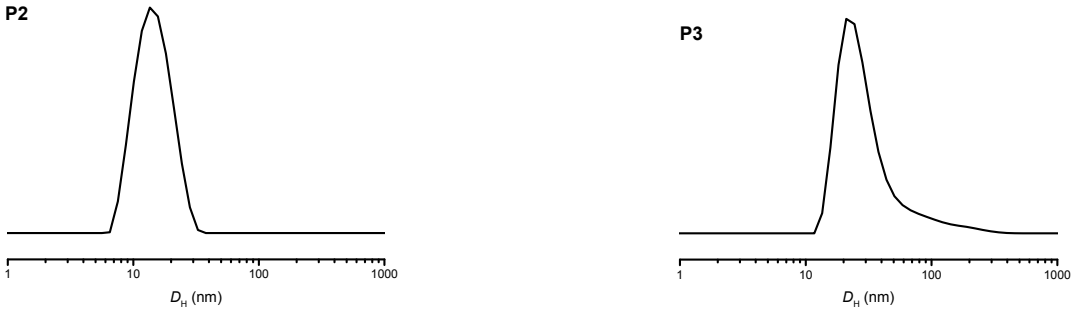

Figure S6 DLS intensity distributions plots for **P2** (left) and **P3** (right) measured at room temperature.

Supporting References.

1) T. Mes, *PhD Thesis*, Eindhoven University of Technology, Eindhoven, the Netherlands, 2011, DOI: 10.6100/IR718881.

2) C. Tansakul, E. Lilie, E. D. Walter, F. Rivera III, A. Wolcott, J. Z. Zhang, G. L. Millhauser and R. Braslau, *J. Phys. Chem. C*, 2010, **114**, 7793–7805.

3) S. B. L. Vollrath, D. Fürniss, U. Schepers and S. Bräse, *Org. Biomol. Chem*., 2013, **11**, 8197–8201.

4) R. M. Hensarling, V. A. Doughty, J. W. Chan and D. L. Patton, *J. Am. Chem. Soc.*, 2009, **131**, 14673–14675.

5) P. J. M. Stals, M. A. J. Gillissen, T. F. E. Paffen, T. F. A. de Greef, P. Lindner, E. W. Meijer, A. R. A. Palmans and I. K. Voets, *Macromolecules*, 2014, **47**, 2947–2954.

6) B. D. Armstrong, S. Han, *J. Am. Chem. Soc.,* 2009, **131(13)**, 4641–4647.

7) J. M. Franck, A. Pavlova, J. A. Scott, and S. Han, *Prog. Nucl. Mag. Res. Sp.*, 2013, **74(C)**, 33–56.

8) K. H. Hausser, D. Stehlik, *Adv. Magn. Reson.* 1968, **3**, 79-139.

9) B. D. Armstrong, S. Han, *J. Chem. Phys.,* 2007, **127**, 104508.

10) B. H. Robinson, D. A. Haas, and C. Mailer, *Science*, 1994, **263**, 490-493.

11) C. Y. Cheng, S. Han, *Annu. Rev. Phys. Chem.*, 2012, **64(1)**, 507-532.

12) C. Y. Cheng, J. Varkey, M. R. Ambroso, R. Langen, and S. Han, *Proc. Natl. Acad. Sci. U. .S A.*, 2013, **110**, 16838–16843.

13) J. M. Franck, M. Sokolovski, N. Kessler, E. Matalon, M. Gordon-Grossman, S. Han, D. Goldfarb, and A. Horovitz, *J. Am. Chem. Soc.,* 2014, **136 (26)**, 9396–9403.

14) J. M. Franck, J. A. Scott, and S. Han, *J. Am. Chem. Soc.*, 2013, **135(11)**, 4175–4178.

15) R. Kausik, S. Han, S. *Phys. Chem. Chem. Phys.*, 2011, **13**, 7732–7746.

16) L. P. Hwang, J. H. Freed, *J. Chem. Phys.,* 1975, **63**, 4017– 4025

17) C. F. Polnaszek, R. G. Bryant, *J. Chem. Phys.,* 1984, **81**, 4038– 4045

18) R. Kausik, S. Han, *J. Am. Chem. Soc.,* 2009, **131**, 18254– 18256

19) B. D. Armstrong, J. Choi, C. Lopez, D. A. Wesener, W. Hubbell, S. Cavagnero, and S. Han*., J. Am. Chem. Soc.,* 2011, **133**, 5987– 5995

20) S. Hussain, J. M. Franck, and S. Han, *Angew. Chem., Int. Ed.,* 2013, **52**, 1953–1958

21) J. M. Franck, Y. Ding, K. Stone, P. Z. Qin, S. Han, *J. Am. Chem. Soc.*, 2015, **137**, 12013–12023.

22) J.S. Hwang, R. P. Mason, L. P. Hwang, J. H. Freed, *J. Phys. Chem.*, 1975, **79**, 489-511.

23) D. E. Budil, S. Lee, S. Saxena, J. H. Freed, *J. Magn. Reson. Ser. A*, 1996, **120**, 155-189.

24) E. Meirovitch. A. Nayeem, J. H. Freed, *J. Phys. Chem.*, 1984, **88**, 3454-3465.

25) L. Columbus. T. Kalai, J. Jeko, K. Hideg, W. L. Hubbell, *Biochemistry*, 2001, **40**, 3828-3846.

26) T. Terashima, T. Sugita, K. Fukae and M. Sawamoto, *Macromolecules*, 2014, **47**, 589–600.

27) L. Rintoul, A. S. Micallef and S. E. Bottle, *Spectrochimica Acta Part A*, 2008, **70**, 713–717.

28) H. Li, Q. Zheng and C. Han, *Analyst*, 2010, **135**, 1360–1364.

29) P. J. M. Stals, J. F. Haveman, R. Martín-Rapún, C. F. C. Fitié, A. R. A. Palmans and E. W. Meijer, *J. Mater. Chem.*, 2009, **19**, 124–130.